REFERENCES

Armor, N.J. Membrane catalysis: where is it now, what needs to be done?. Catal. Today 25 (1995): 199-207.

Armor, N.J. Application of catalytic inorganic membrane reactors to refinery products. J. Memb. Sci. 147 (1998): 217-233.

Balachandran, U. Ceramic membrane reactor converting methane to syngas. Catal. Today 36 (1997): 265-272.

Barbieri, G. and Vittorio, V. Methan stream reforming analysis in a Pd-based catalytic membrane reactor. Ind. Chem. Eng. Res. 36 (1997): 3369-3374.

Barias, O.A., Holmen, A. and Blekkan, E.A. Propane dehydrogenation over supported platinum catalysts - effect of tin as a promoter. Catal. Today 24 (1995): 361-364.

Barias, O.A., Holmen, A. and Blekkan, E.A. Propane dehydrogenation over supported Pt and Pt-Sn catalysts: Catalyst preparation, characterization, and activity measurements. J. Cat. 158 (1996): 1-12.

Bindjouli, A.B., Dehocche, Z. and Bernauer, B. Numerical simulation of catalytic inert membrane reactor. Computers. chem. Engng. 18 (1994): s337-s341.

Casanave, D., Fialy, K. and Dalmon. Computer-aided optimization of the catalytic dehydrogenation in packed-bed membrane reactor. Computers.chem. Engng. 22 (1998), s691-s694.

Champagnie, A. The study of ethane dehydrogenation in a catalytic membrane reactor. J. Catal. 134 (1993): 613-619.

Collins, J. and Brinker, C.J. catalyst dehydrogenation of propane in hydrogen permselective membrane reactor. Ind. Chem. Eng. Res. 35 (1996): 4398-4405.

Coronas, J., Menendez, M. and Santamaria, J. Methan oxidative coupling using porous ceramic reactor. Part II, Reaction studies. Chem. Engng. Sci. 49 (1994a): 2015-2025.

Coronas, J., Menendez, M.and Santamaria, J. Development of ceramic membrane reactors with non-uniform permeation pattern. Application to methane oxidative coupling. Chem. Engng. Sci. 49 (1994b): 4749-4757.

Coronas, J., Menendez, M. and Santamaria, J. Use of a ceramic membrane reactor for oxidative dehydrogenation of ethane to ethylene and higher hydrocarbons. Ind. Chem. Eng. Res. 34 (1995): 4229-4757.

Demiguel, S.R., Castro, A.A., Scelza, O.A. and Soria, J. Effect of the addition of alkali-metals on the metallic phase of Pt/Al_2O_3 catalysts. Cat. Letts. 32 (1995): 281-291

Fogler, H.G. Elements of chemical reaction engineering. (n.p.): Prentice-Hall International, Inc. 2nd (1992): 543-635.

Froment, G.F. and Bischoff, K.B. Chemical reactor analysis and design. (n.p.): John Wiley & Sons (1990):125-167

Galuszka, J., Pandey, R. and Ahmed, S., Proceeding of Fifth European Workshop on Methan Activation. Limerick. Ireland. (June1997).

Gobina, E., Hou, K. and Hung, R. Mathematical analysis of ethylbenzene dehydrogenation comparison of microporous and dense membrane system. J. Memb. Sci. 105 (1995): 163-176.

Gobina, E. and Hughes, R. Reaction assisted hydrogen transport during catalytic dehydrogenation in a membrane reactor. Appl. Cat. 137 (1996): 119-127.

Gobina, E. and Hughes, R. Reaction coupling in a catalytic membrane reactor. Chem. Eng. Sci.137 (1996): 3045-3050.

Govind, R. and Atnoor, D. Development of a composite Pd membrane for selective hydrogen separation at high temperature. Ind. Chem. Eng. Res. 30 (1991): 591-594.

Gryaznov, V.M. and Slin'ko, M.G. Selectivity in catalysis by hydrogen-porous membranes. Discuss. Faraday. Soc., 72 (1982): 73-93.

Gryaznov, V.M. Hydrogen permeable palladium membrane catalysis. Plat. Met. Rev., 30 (1986): 68-72.

Gryaznov, V.M. Membrane catalysis. Catal. Today. 51 (1999): 391-395.

Guo, X.M., Hidajat, K.and Ching, C.B. Oxidative coupling of methane in a solid oxide membrane reactor. Ind. Chem. Eng. Res. 36 (1997): 3576-3582.

Hsieh, H.D. Inorganic Membrane for Separation and Reaction. Amsterdam: Elsevier, (1996), 620 pp.

Itoh, N. A membrane reactor using Pd AIChE. J. 33 (1987): 1576-1580.

Itoh. N., Xu, W.C. and Sathe, A.M. Capability of permeate hydrogen through Pd-based membranes for acetylene hydrogenation. Ind. Chem. Eng. Res. 32 (1993): 2614-2619.

Itoh, N., Xu, W.C. and Haraya, K. Radial mixing diffusion of hydrogen in a packed-bed type of Pd membrane reactor. Ind. Chem. Eng. Res. 33 (1994): 197-202.

Kikuchi, E. Palladium/ceramic membranes for selective hydrogen permeation and their application to membrane reactor. Catal.Today. 25 (1995): 333-337.

Koukou, M.K., Papayannakos, N. and Markatos, N.C. Dispersion effect on Membrane reactor performance. AIChE. J. 42 (1996): 2607-2615.

Krishnamurthy K.R. Modifications in supported metal catalysts: Effect of promoters. Recent Advances in Basic and Applied Aspects of Industrial Catalysis. 113 (1998): 139-150

Lafarga, D., Santamaria, J. and Menendez, M. Methane oxidative coupling using porous ceramic membrane reactors, Part I, reactor development. Chem. Eng. Sci 49 (1994): 2005-2013.

Lambert, C.K. and Gonzalez, R.D. Activity and selectivity of a Pd/Al2O3 catalyst membrane in the partial hydrogenation reation of acetylene and 1,3-butadiene. Cat. Letter. 57 (1999): 1-7.

Larsson M, Henriksson, N. and Andersson, B. Investigation of the kinetics of a deactivating system by transient experiments. App. Cat. A. 166 (1998): 9-19.

Larsson M, Henriksson, N. and Andersson, B. Estimation of reversible and irreversible coke by transient experiments. Catalyst Deactivation. 111(1997): 673-680.

Levenspiel, O. Chemical reaction engineering. (n.p.): John Wiley & Sons. 2nd (1972): 462-477.

Liu, C., Xu, Y. and Liao, S. Mono- and bimetallic catalytic hollow-fiber reactors for the selective hydrogenation of butadiene in 1-butene. App. Cat. A.172 (1998):23-29.

Maksuda, T., Koike, I. And Kikuchi, E. Dehydrogenation of isobuthane in a Pd membrane reactor. Appl. Cat. A. 96 (1993): 3-10.

Nozaki, T.and Fujimoto, K. Oxide ion transport for selective oxidative coupling of methan with new membrane reactor. AIChE. J. 40 (1994): 870-877.

Pantazidis, A., Dalmon, J.A. and Miromatos, C. Oxidative dehydrogenation of propane on catalytic membrane reactor. Cat. Today. 25 (1994): 403-408.

Praserthdam P., Mongkhonsi, T., Kunatippapong, S., Jaikaew, B. and Lim, N. Determination of coke deposition on metal active sites of propane dehydrogenation catalysts. Catalyst Deactivation. 111 (1997): 153-158.

Raich, B.A. and Foley, H. Supra-equilibrium conversion in palladium membrane reactors: Kinetic sensitivity and time dependence. Appl. Catal. A. 129 (1995):167-188.

Saracco, G., Neomagus, H.W.J.P. and Versteeg, G.E., High-temperature membrane reactor: Potential and problems. Chem. Engng. Sci. 54 (1999): 1997-2017.

Schramm, O. and Andreas, S. Comparing porous and dense membranes for the application in membrane reactors. Chem. Eng. Sci. 54 (1999): 1447-1453.

Sheintuch, M. and Dessau, R.M. Observation, modeling and optimization of yield, selectivity and activity during dehydrogenation of isobuthane and propane in a Pd membrane reactor. Chem. Eng. Sci. 51 (1996): 535-547.

Sherman, J.X and Thomson, W.J., Perovskite-type oxide membranes for the oxidative coupling of membrane. AIChE. J. 43 (1997): 2731-2740.

Shigeyuki, U. and Noboru, S. Stream Reforming of methane in a hydrogen-permeable membrane reactor. App. Cat. 67 (1991): 223-230.

Shu, H.D. and Grandjean, P.B. Catalytic palladium-based membrane reactor. Can. Chem .Engng. 75 (1991): 712-72.

Ten Elshof, J.E., Bouwmeester, H.J.M. and Verweeij, H., Oxidative coupling of membrane in a mixed-conductive perovskite membrane reactor. Appl. Catal. A. 130 (1995): 195-212.

Tonovich, A.L.Y., Zilka, J.L. and Jeminez, D.M. Experimental investigations of Inorganic membrane reactor. A distributed feed approach for partial oxidation reaction. Chem. Engng. Sci. 51 (1996b): 789-806.

Uemiya, S., Sato, N. and Anto, N., Stream reforming of methanol in a hydrogen permeable membrane reactor. Appl. Catal. 67 (1991): 223.

Ward, T.L. and Dao, T. Model of hydrogen permeation behavior in palladium membranes. J. Memb. Sci. 153 (1999): 211-231.

Weyten H, Keizer K and Kinoo A. Dehydrogenation of propane using a pack-bed catalytic membrane reactor. AIChE J. 43 (1997): 1819-1827.

Xu, S.J. and Thomson. W.J. Perovskite-type oxide membrane for the oxidative coulping of methane. AIChE. J. 43 (1997): 2731-2740.

Yildirim, Y., Gobina, E. and Hughes, R., An experimental evaluation of high-temperature composite membrane systems for propane dehydrogenation. J. Mem. Sci.135 (1997): 107-115.

Zaman, J. and Chakma, A. Inorganic membrane reactor. J. Memb. Sci. 94 (1994) : 1-28

Zhao, R. and Govind, R. Studies on Pd membrane reactor for dehydrogenation reaction. Sep. Sci. Tech. 25 (1990), 1473-1488.

Ziaka, Z.D., Minet, R.G. and Tsotsis, T.T. A High-temperature catalytic membrane reactor for propane dehydrogenation. J. Mem. Sci. 77 (1993): 221-232.

APPENDICES

APPENDIX A
SAMPLE OF CALCULATION FOR CATALYST PREPARATION

The sample of calculation shown below is for 0.3 wt.% Pt- 0.3 wt.% Sn- 0.6 wt.% K/γ-Al$_2$O$_3$ catalyst. The hydrochloric acid is added to the impregnating solution by 5 wt % of the alumina support. The alumina support weight used for all preparation is 2 grams.

If X grams of alumina support is used, so each 100 grams of the catalyst is composed of :

Platinum	0.3	g
Tin	0.3	g
Potassium	0.6	g
Hydrochloric acid	0.05 x X	g
Alumina support	X	g
then 0.3 + 0.3 + 0.6 + (0.05xX) + X	= 100	g
X	= 94.0952	g

The platinum compound is from chloroplatinic acid (H$_2$PtCl$_6$.6H$_2$O), whose molecular weight is 517.92 and the platinum content in the compound is 37.67 wt %. The stock solution of chloroplatinic acid has the concentration of 1 g in 25 ml. of water.

The tin compound is from stannous chloride dihydrate (SnCl$_2$.2H$_2$O) whose molecular weight is 118.69 and the tin content in the compound is 51.02 wt.%.

The potassium compound is from potassium nitrate (KNO$_3$) where molecular weight is 101, and potassium content is 38.61 wt.%. The stock solution of potassium nitrate has the concentration 3 g in 25 ml. of water.

Concentration of hydrochloric acid solution is 37 % volume by volume, its density is 1.19 kilogram per liter.

The calculation procedures of the amount of each ingredients for the required composition of the 0.3 wt.% Pt- 0.3 wt.% Sn- 0.6 wt.% K catalyst are as follows.

For two grams of alumina support used :

1) Platinum required = (0.3x2)/94.10) g

= 6.37×10^{-3} g

Chloroplatinic acid required = 6.37×10^{-3}x100x25/37.67 ml

= 0.4232 ml

2) Tin required = 2x0.3/94.0952 g

= 6.376×10^{-3} g

Stannous chloride dihydrate required

= 6.376×10^{-3}x100/51.02 g

= 0.0125 g

3) Potassium required = 2x0.6/94.0952 g

= 0.0128 g

Potassium nitrate required = 0.0128x100x25/(38.61x3) ml

= 0.2763 ml

4) Hydrochloric and solution required

= 2x0.05 g

= 0.1 g

The amount of hydrochloric and by volume

= 0.1/(1.190x0.37) ml

= 0.2271 ml

As the pore volume of the alumina support is 1 ml/g, the total volume of impregnating solution that must be used is 2 ml by the requirement of dry impregnation method, the de-ionized water is added until the volume of impregnating solution is 2 ml as equal to the volume of the alumina pore volume.

APPENDIX B

CALCULATION OF METAL ACTIVE SITES

The calculation of the number of metal active sites of the catalyst by CO adsorption at room temperature has the procedure as follows :

Let:

Weight of catalyst used	= w	kg
Height of CO peak after adsorption	= A	unit
Height of 40 μl. standard CO peak	= B	unit
Amounts of CO adsorbed on catalyst	= B-A	unit
Volume of CO adsorbed on catalyst	= [(B-A)/B](40)	μl
Volume of gas 1 mole at 30 °C	= 24.86x10^6	μl
Moles of CO adsorbed on catalyst	= [(B-A)/B][40/24.86x10^6]	mole

Molecules of CO adsorbed on catalyst

$$= 1.61 \times 10^{-6}[\{B\text{-}A)/B](6.02 \times 10^{23}) \quad \text{molecules}$$

$$\text{Number of metal active sites} = \frac{9.68 \times 10^{17}[(B-A)/B]}{W} \quad \text{molecules of CO/kg}_{cat.}$$

APPENDIX C

CALCULATION OF DIFFUSIONAL LIMITATION EFFECT

The two types of diffusion resistances which affect overall rate of reaction are (1) *external resistance:* diffusion of reactants or products between the bulk fluid and the external surface of catalyst, and (2) *internal resistance:* diffusion of reactants or products from the external pellet surface (pore mouth) to the interior of the pellet. The recent procedures of external and internal resistance calculations are summarized by Froment *et al.*, (1990), Fogler, (1992) and Levenspie, (1972).

External mass transfer

Let a component A of a fluid reacts on active centers at the surface of a catalyst. It is convenient for the present to define a rate based on the interfacial surface area ($r_A^{''}$), and assume that it is first order:

$$r_A^{''} = k_s C_{As} \qquad (C-1)$$

The consumption of A at the interface has to be compensated by transport from the bulk fluid, the flux of which can be written as

$$N_A = k_g \left(C_A - C_{As} \right) \qquad (C-2)$$

For steady state, the two terms must be equal. Mass transfer coefficient of A through stagnant film of reaction mixture (k_g), for which the film theory gives:

$$k_g = \frac{k_g^0}{p_{fA}} \qquad (C-3)$$

where k_g^0 = mass transfer coefficient for the case of equimolar counterdiffusion

p_{fA} = film pressure factor $= \dfrac{(1 + \delta p_A) - (1 + \delta p_{As})}{\ln \dfrac{(1 + \delta p_A)}{(1 + \delta p_{As})}} \qquad (C-4)$

Then, thecorrelation of the mass transfer coefficients can be presented in term of the j_D factor

$$j_D = \frac{k_g^0 Mw_m}{G} Sc^{2/3}$$

$$= \frac{k_g Mw_m P_{fA}}{G} Sc^{2/3} = f(\text{Re}) \qquad\qquad (C\text{-}5)$$

Calculation data

Reactant	=	3% Propane/Nitrogen	
Temperature	=	773	K
Pressure	=	10^5	Pa
Feed flow rate	=	1×10^{-6}	m^3/s
Catalyst diameter	=	0.214×10^{-3}	m
Catalyst weight	=	0.2×10^{-3}	kg
Catalyst density	=	1500	kg/m^3
Conversion	=	30	%

Feed composition

Species	fraction
Propane	0.03
propylene	0
Hydrogen	0.03
Nitrogen	0.94

Propane molar flow rate (F_{AO}) $\quad = \dfrac{1\times10^{-6}\times0.03}{82\times10^{-3}\times303} = 1.2\times10^{-9}$ $\qquad$ kmol/s

Propane mass flux(G) $\quad = \dfrac{1.2\times10^{-9}\times44}{\pi\times\left(\dfrac{0.006}{2}\right)^2} = 1.88\times10^{-3}$ $\qquad$ kg/m^{2}s

External surface area per catalyst particle $= \pi(2.14\times10^{-4})^2 = 1.44\times10^{-7}$ m^2/particle

Weight per catalyst particle $\quad = \dfrac{\pi(2.14\times10^{-4})^3 \times1400}{6} = 7.29\times10^{-9}$ kg$_{cat}$/particle

External surface area per weight catalyst $(a_m) = \dfrac{1.44\times10^{-7}}{7.29\times10^{-9}} = 19.9$ $\qquad$ m^2/kg$_{cat}$

Composition of the reaction mixture

Propane: $\dfrac{y_{AO}(1-X)}{1+y_{AO}X}P_T = \dfrac{0.03\times(1-0.3)}{1+0.03\times0.3}\times10^5$ = 2.05 x 10^3 Pa

Propylene: $\dfrac{y_{AO}(\Theta_B+X)}{1+y_{AO}X}P_T = \dfrac{0.03\times0.3}{1+0.03\times0.3}\times10^5$ = 8.91 x1 0^2 Pa

Hydrogen: $\dfrac{y_{AO}(\Theta_C+X)}{1+y_{AO}X}P_T = \dfrac{0.03\times(1+0.3)}{1+0.03\times0.3}\times10^5$ = 3.89 x 10^3 Pa

Nitrogen: $\dfrac{y_{AO}\Theta_I}{1+y_{AO}X}P_T = \dfrac{0.03\times31.33}{1+0.03\times0.3}\times10^5$ = 9.31 x 10^4 Pa

Estimation of viscosity

Use the Lennard-Jones potential:

$$\mu_i = 2.669x10^{-5}\frac{\sqrt{MwT}}{\sigma^2\Omega}$$

Species	Mw	σ	ε/K	Ω	μ_i x10^7[kg/m·s]
Propane	44.09	5.11	237.1	0.928	2.027
Propylene	42.08	4.67	298.9	0.999	2.202
Hydrogen	2.01	2.87	59.7	0.718	1.836
Nitrogen	28.02	3.79	71.4	0.734	3.710

Viscosity, molecular weight, density of gases mixture

$\mu_m = \sum\limits_{i=1}^{n}y_i\mu_i$ = $(2.05x10^{-2}$ x $2.027x10^{-7}) + (8.91x10^{-3}$ x $2.202x10^{-7}) +$

$(3.89x10^{-2}$ x $1.836x10^{-7})+ (0.93$ x $3.710x10^{-7})$

= $3.59x10^{-7}$ kg/m·s

$Mw_m = \sum\limits_{i=1}^{n}y_iMw_i$ = $(2.05x10^{-2}$ x $44.09)+ (8.91x10^{-3}$ x $42.08)+$

$(3.89x10^{-2}$ x $2.01)+ (0.93$ x $28.02)$

= 27.46 kg/kmol

$\rho_m = \dfrac{Mw_iT_O}{V_OT}$ = $\dfrac{28.206x273}{22.4x773}$

= 0.44 kg/m^3

Diffusion coefficients

For the correlation of Fuller-Schettle-Griddings:

$$D_{12} = 10^{-3} \frac{T^{1.75}\left(1/Mw_1 + 1/Mw_2\right)^{1/2}}{P_T\left[\left(\sum_i V_{i1}\right)^{1/3} + \left(\sum_i V_{i2}\right)^{1/3}\right]^2}$$

No.	Species	Diffusion volume of molecule	Binary diffusion coefficient of 1 in other species x10^5 [m^2/s]
1	Propane	65.34	-
2	propylene	61.38	3.88
3	Hydrogen	7.07	23.31
4	Nitrogen	17.9	6.26

Diffusion coefficient of component i in reaction mixture

$$\frac{1}{D_{im}} = \frac{1}{1+y_j} \sum_{k \neq j}^{n} \frac{1}{D_{jk}}\left(y_k + y_j \frac{\alpha_k}{|\alpha_j|}\right)$$

$$D_{Am} = \left[\frac{1}{1+y_A}\left(\frac{y_B + y_A}{D_{AB}} + \frac{y_C + y_A}{D_{AC}} + \frac{y_I}{D_{AI}}\right)\right]^{-1}$$

$$= \left[\frac{1}{1+2.05\times10^{-2}}\left(\frac{8.91\times10^{-3} + 2.05\times10^{-2}}{3.88\times10^{-5}} + \frac{3.89\times10^{-2} + 2.05\times10^{-2}}{23.31\times10^{-5}} + \frac{0.93}{6.26\times10^{-5}}\right)\right]^{-1}$$

$$= 6.29 \times10^{-5}\, \text{m}^2/\text{s}$$

Schmidt and Reynolds number

$$Sc = \frac{\mu_m}{\sigma_m D_{Am}} \quad = \quad \frac{3.59\times10^{-7}}{0.44\times6.29\times10^{-5}} \quad = \quad 1.32\times10^{-2}$$

$$Re = \frac{d_p G}{\mu_m} \quad = \quad \frac{0.214\times10^{-3}\times1.88\times10^{-3}}{3.59\times10^{-7}} \quad = \quad 1.13$$

Since Re<190, the following j_D (Eq.C-5) correlation should be used:

$$j_D = 1.66(Re)^{-0.51} = 1.66(1.13)^{-0.51} \quad = \quad 1.56$$

Reaction rate constant is used in the simple form:

$$r_A = \frac{F_{AO}X}{W_{cat}} = \frac{1.2\times10^{-9}\times0.3}{0.0002} = 1.81\times10^{-6} \quad \text{kmol/kg}_{cat}\,\text{s}$$

Now the partial pressure drop can be calculated. Assuming that $\Delta p_A = 0$, the film pressure factor for a reaction (Eq.C-4) becomes:

$$p_{fA} = p_T + \delta_A p_A \qquad = 1 + 2.05 \times 10^{-2} = 1.0205 \text{ bar} = 1.0205 \times 10^5 \text{ Pa}$$

$$\Delta p_A = \frac{r_A M w_m p_{fA}}{a_m G j_D}(Sc)^{2/3} = \frac{1.81 \times 10^{-6} \times 27.46 \times 1.0205}{19.9 \times 1.88 \times 10^{-3} \times 1.56}\left(1.32 \times 10^{-2}\right)^{2/3}$$

$$= 4.84 \times 10^{-5} \text{ bar}$$

Substitution of this estimate for Δp_A in Eq. C-4 , written in terms of partial pressures

$$p_{fA,2} = \frac{4.48 x 10^{-5}}{\ln(1.0205 / 1.0204)} = 1.0207$$

The new estimate for the film pressure factor may be considered sufficiently close to the starting value 1.0205, so that no further iterations on Δp_A.

Summary

The partial pressure difference of propane between catalyst surface and bulk fluid for kinetic study and membrane reactor studies are shown in Table C-1 and C-2, respectively.

Table C-1 Partial pressure difference of propane between catalyst surface and bulk gas of 3% propane at 773 K and GHSV 12,700 h^{-1}: kinetic study condition.

Feed molar flow rate x 10^7 (m^3/s)	Propane partial pressure difference (%)
2.5	0.467
5.0	0.339
7.5	0.278
10.0	0.242

Table C-2 Partial pressure difference of propane between catalyst surface and bulk gas of 3% propane at 773 K and GHSV 90 h^{-1}: membrane reactor study condition.

Temperature (K)	Propane partial pressure difference (%)
723	0.0689
773	0.0773
823	0.0846
873	0.1014

Internal mass transfer

Considering the simplest case of the first-order reaction, equimolar counterdiffusion isothermal conditions and the simplest geometry of a slab of catalyst when the y-coordinate is oriented from the center line to the surface, the steady-state diffusion equation is

$$D_{eA} \frac{d^2 C_A}{dy^2} - k_W \rho_s C_A = 0 \qquad \text{(C-6)}$$

With the boundary conditions

$$C_A(L_p) = C_A^s \qquad \text{at the surface}$$

$$\frac{dC_A(0)}{dy} = 0 \qquad \text{at the center line}$$

The solution of Eq.C-6 is

$$\frac{C_A(y)}{C_A^s} = \frac{\cosh \sqrt{\frac{k\rho_s}{D_{eA}}} y}{\cosh \sqrt{\frac{k\rho_s}{D_{eA}}} L} \qquad \text{(C-7)}$$

Thiele (1939) who defined the effectiveness factor:

$$\eta = \frac{\text{rate of reaction with pore diffusional resistance}}{\text{rate of reaction with surface condition}}$$

Thus, the actual reaction rate that would be observed is

$$(r_A)_{obs} = \eta r_A C_A^s \qquad \text{(C-8)}$$

From the solution of above differential equation (concentration profiles) and the definition of effectiveness factor, the effectiveness factor will be obtained:

$$\eta = \frac{\tanh \phi'}{\phi'} \qquad \text{(C-9)}$$

where ϕ' is Thiele modulus $= L\sqrt{k\rho_s D_{eA}} \qquad \text{(C-10)}$

From Eq.C-9 and C-10 leading to:

$$r_A \rho_s = \eta \frac{\phi^2}{L^2} D_{eA} C_A^s$$

If all the directly observable quantities are put on the one side of equation:

$$\frac{(r_A \rho_s)_{obs} L^2}{D_{eA} C_A^s} = \eta \phi^2 = \Phi \qquad (C-11)$$

From the effectiveness factor versus Thiele modulus curve (Figure C-1), The following condition are obtained

1. For $\phi \ll 1, \eta = 1$ (no pore diffusion limitation), and so

        R.H.S. = $\phi^2 \ll 1$

2. For $\phi \gg 1, \eta = 1/\phi$ (strong pore diffusion limitation) and so

        R.H.S. = $1/\phi \times \phi^2 \gg 1$

Thus the criterion for negligible pore diffusion limitation is

$$\Phi = \frac{(r_A \rho_s)_{obs} L^2}{D_{eA} C_A^s} \ll 1$$

In this case, three types of catalyst sizes of 60/80, 200/250 and 250/325 were used to determine the values Φ as shown in Table C-3. From the result, it was found that the effect of internal mass transfer for all catalyst size could be ignored.

Table C-3 Diffusional limitation term (Φ) on different catalyst size of 3%propane at773K and GHSV 12,700 h^{-1}

Catalyst size (mesh)	60/80	200/250	250/325
Φ	1.42×10^{-4}	1.35×10^{-5}	8.20×10^{-6}
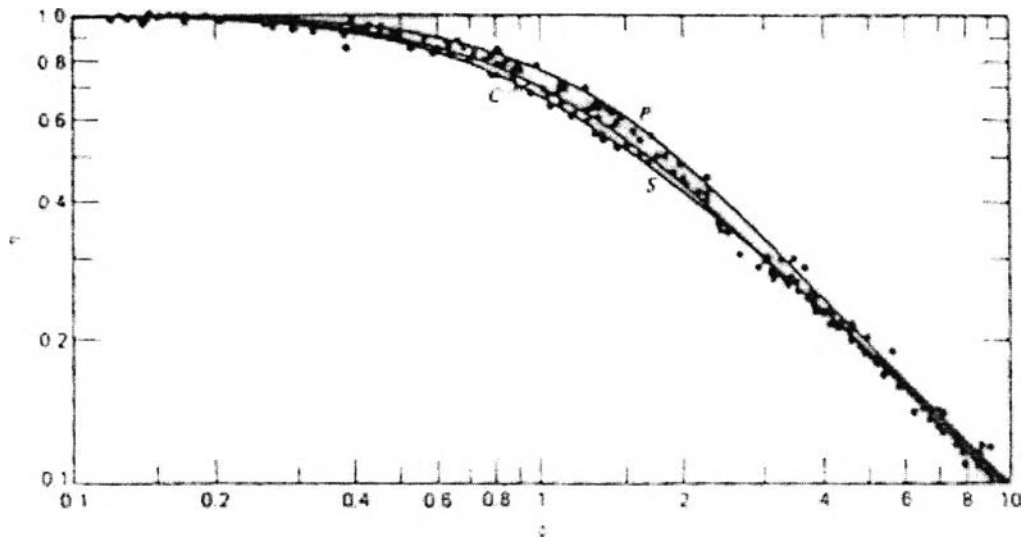
Figure C-1 Effectiveness factor for slap (P), cylinder (C) and sphere (S) as function of the Thiele modulus (Froment, 1990).

APPENDIX D

DETERMINATION OF REACTION RATE CONSTANT

Assuming plug flow and steady state condition, the material balance of a plug flow reactor can be made as fallows

$$F_A|_z - F_A|_{z+\Delta z} = r_A A_C \Delta Z \tag{D-1}$$

$$\frac{dF_A}{dV} = -r_A \tag{D-2}$$

Eq. (D-2) can be rearranged using of catalyst weight as a basis to obtain.

$$\frac{dF_A}{dW_{cat}} = -r_A' \tag{D-3}$$

where $F_A = F_{AO}(1 - X)$
or $dF_A = -F_{AO}dX$ then Eq.D-3 becomes

$$\frac{dX}{d\left(\dfrac{W_{cat}}{F_{AO}}\right)} = r_A' \tag{D-4}$$

For the whole reactor the expression must be integrated. Now F_{A0}, the feed rate, is constant, but r_A' is certainly dependent on the partial pressures or conversion.

$$\frac{W_{cat}}{F_{AO}} = \int_0^X \frac{dX}{r_A'} \tag{D-5}$$

In this case, the rate of reaction is assumed to be a in simple form with k_{app} as reaction rate constant based of catalyst weight.

$$r_A' = k_{app}\left(p_{C_3H_8} - \frac{p_{C_3H_6} p_{H_2}}{K_{eq}}\right) \tag{D-6}$$

Table D-1 Composition of the reaction mixture:

Species	Feed rate	Change rate	Effluent rate	Partial pressure
Propane	F_{AO}	$-F_{AO}X$	$F_{AO}(1-X)$	$\dfrac{y_{AO}(1-X)}{1+y_{AO}X}P_T$
Propylene	$\Theta_B F_{AO}$	$F_{AO}X$	$F_{AO}(\Theta_B+X)$	$\dfrac{y_{AO}(\Theta_B+X)}{1+y_{AO}X}P_T$
Hydrogen	$\Theta_C F_{AO}$	$F_{AO}X$	$F_{AO}(\Theta_C+X)$	$\dfrac{y_{AO}(\Theta_C+X)}{1+y_{AO}X}P_T$
Nitrogen	$\Theta_I F_{AO}$	—	$\Theta_I F_{AO}$	$\dfrac{y_{AO}(1-X)}{1+y_{AO}X}P_T$

From the simple rate expression and the composition of the reaction mixture as shown in Table D-1, the rate constant base of catalyst weight, k_{app}, can be obtained:

$$k_{app} = \frac{F_{AO}}{W_{cat}} \int_0^{X_A} \frac{dX}{\left(\dfrac{p_{AO}(1-X)}{1+y_{AO}X} - \dfrac{p_{AO}^2(\Theta_B+X)(\Theta_C+X)}{(1+y_{AO}X)^2 K_{eq}} \right)} \qquad \text{(D-7)}$$

APPENDIX E
DETERMINATION OF EQUILIBRIUM CONSTANT AND EQUILIBRIUM CONVERSION

Dehydrogenation of propane is an equilibrium limited reaction. The maximum extent of certain reaction is governed by thermodynamic equilibrium. Maximum conversion of the propane to propylene is calculated at given operating temperature, pressure and feed composition according to the laws of thermodynamic.

Equilibrium constant

Standard free energy change can be expressed as:

$$\Delta G^0 = \Delta H^0 - T\Delta S^0$$
$$= \Delta H^0 - T\left(-\frac{d\Delta G^0}{dT}\right) \tag{E-1}$$

where
$$\Delta S^0 = -\frac{d\Delta G^0}{dT} \tag{E-2}$$

Combination Eq.E-1 and E-2, we see relation between free energy and enthalpy of reaction:

$$\Delta H^0 = -RT^2 \frac{d\left(\Delta G^0/RT\right)}{dT} \tag{E-3}$$

$$-\frac{\Delta H^0}{RT^2}dT = d\frac{\Delta G^0}{RT}$$

The enthalpy of reaction at any temperature can be written in the term of enthalpy of reaction at reference temperature and heat capacity, Eq.(E-5).

$$\Delta H_T^0 = \Delta H_{298}^0 + \int_{298}^{T} \Delta C_p^* dT \tag{E-4}$$

where
$$C_p^* = \Delta a + \Delta bT + \Delta cT^2 + \Delta dT^3 \tag{E-5}$$

$$\Delta a = \sum_{i=1}^{n} v_i a_i ; \quad \Delta b = \sum_{i=1}^{n} v_i b_i ; \quad \Delta c = \sum_{i=1}^{n} v_i c_i ; \quad \Delta d = \sum_{i=1}^{n} v_i d_i \tag{E-6}$$

The exact form for the dependence of the free energy of reaction on temperature is :

$$\int_{298}^{T} \frac{d\Delta G^0}{RT} = -\frac{1}{R}\int_{298}^{T} \frac{\Delta H^0}{T^2}dT \tag{E-7}$$

Substitute Eq.E-4, E-5 and E-6 in E-7 and the integrated result are obtained:

$$\Delta G_T^0 = B_1 - \Delta a \ln T - \frac{\Delta b}{2}T^2 - \frac{\Delta C}{6}T^3 - \frac{\Delta d'}{12}T^4 - B_2 RT \tag{E-8}$$

where $B_1 = \Delta H_{298}^0 - (\Delta a \times 298) - \left(\frac{\Delta b}{2} \times 298^2\right) - \left(\frac{\Delta c}{3} \times 298^3\right) - \left(\frac{\Delta d}{4} \times 298^4\right)$

$B_2 = \frac{1}{R}\left(\frac{B_1}{298} - \Delta a \ln 298 - \frac{\Delta b}{2} \times 298 - \frac{\Delta c}{6} \times 298^2 - \frac{\Delta d}{12} \times 298^3 - \frac{\Delta G_{298}^0}{298}\right)$

Table G-1 Heat of formation, free energy of change at reference state (298 K) and heat capacity parameters.

Species	ΔH_{298}^0 [kcal/mol]	ΔG_{298}^0 [kcal/mol]	a	$b \times 10^2$	$c \times 10^5$	$d \times 10^9$
Propane	-24.820	-5.614	-0.966	7.279	-3.755	7.580
Propylene	4.879	14.990	0.753	5.691	-2.910	5.880
Hydrogen	-	-	6.424	0.104	-0.0078	-
Δ	29.699	20.604	8.671	-1.634	0.941	-1.9

From Eq.E-8 and data in Table E-1, the standard free energy change of propane dehydrogenation reaction at 773 K can be obtained.

$$\Delta G_{773}^0 = 5243 \quad \text{cal/mol}$$

At constant temperature and pressure, the relationship between free energy change and equilibrium constant is:

$$\Delta G_{T,P}^0 = -RT \ln K \tag{E-9}$$

Thus, $K = e^{-\left(\frac{\Delta G_{T,P}^0}{RT}\right)} = e^{-\left(\frac{5,243}{1.987 \times 773}\right)}$ \qquad (E-10)

$$= 0.0329$$

At constant temperature and pressure, the equilibrium constant is defined as

$$K = \prod y_i^{\upsilon_i} \phi_i^{\upsilon_i} \cdot P^{\upsilon}$$ (E-11)

The operating condition in this study is at 773 K, atmospheric pressure ($\phi_i^{\upsilon_i} \approx 1$), and

$\upsilon=1$. Thus in this studies, the equilibrium constant for propane dehydrogenation can

be reduced to:

$$K = \frac{y_{C_3H_6} y_{H_2}}{y_{C_3H_8}} P$$ (E-12)

Substitution fraction of each species from Table D-1 to Eq.E-12, the equilibriun

constant in term of equilibrium conversion and feed properties are given:

$$K = \frac{F_{A0}\left(\Theta_B + X_{eq}\right)\left(\Theta_C + X_{eq}\right)}{\left(1 - X_{eq}\right)\left(1 + y_{A0} X_{eq}\right)} P$$ (E-13)

Equation E-13 are used to calculate the equilibrium conversion and the result

of free energy change, equilibrium constant and equilibrium conversion at any

operating temperature and feed composition are shown below.

Table E-1 Free energy change, equilibrium constant and equilibrium conversion at
some operating temperature and feed composition

Temperature [K]	ΔG_T^0 [cal/mol]	Equilibrium constant (K)	Equilibrium conversion (X_eq) [%]		
			3 %	20%	50%
723	6898	8.21e-3	40.50	18.61	12.36
773	5243	3.29e-2	63.71	34.05	23.70
823	3584	1.116e-1	82.25	53.57	40.07
873	1925	0.3296	92.43	72.29	59.10

APPENDIX F

HYDROGEN PERMEATION MODEL

A set of differential equations for the permeation of H_2 through a Pd membrane can be derived in both shell and tube sides of a reactor with the assumption shown in Figure F-1, the mass balances can be performed as follow.

Material balance
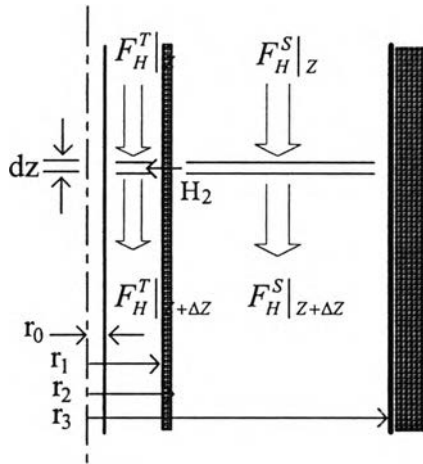
Assumption:

- Steady state operation
- Isothermal operation
- Negligible pressure drop in packed bed
- Negligible radial diffusion effect

Figure F-1 Packed bed reactor

Shell side:

A steady state mol balance on hydrogen species in the reactor segment between z and z + Δz is:

$$F_H^S\big|_z - F_H^S\big|_{z+\Delta z} = 2\pi r_2 \Delta Z J_H \qquad (F\text{-}1)$$

Sieverts's law is used to describe the H_2 transport through the Pd film. Consequently, the H_2 flux is:

$$J_H = \alpha_H \left(\sqrt{p_H^S} - \sqrt{p_H^T}\right) \qquad (F\text{-}2)$$

From the material balance(Eq.F-1) and Sieverts's law, a differential equation (Eq.F-3) can be obtained and can be, further, converted to a dimensionless form (Eq.F-4):

$$\frac{dF_H^S}{dz} = -2\pi r_2 \alpha_H \left(\sqrt{p_H^S} - \sqrt{p_H^T} \right)$$

(F-3)

$$\frac{d\Phi_H^S}{dL} = -c\alpha_H \left(\sqrt{\beta_H^S} - \sqrt{\beta_H^T} \right)$$

(F-4)

where

$$\beta_H^S = \frac{p_H^S}{P_{T,0}^S} = \frac{P_T^S}{P_{T,0}^S} \left(\frac{\Phi_H^S}{\Phi_H^S + \Phi_I^S} \right)$$

$$\beta_H^T = \frac{p_H^T}{P_{T,0}^S} = \frac{P_T^T}{P_{T,0}^S} \left(\frac{\Phi_H^T}{\Phi_H^T + \Phi_I^T} \right)$$

$$C = \frac{2\pi r_2 L \sqrt{P_T^S}}{F_{H,0}^S} \; ; \; \Phi_H^S = \frac{F_H^S}{F_{H,0}^S} \; ; \; \Phi_H^T = \frac{F_H^T}{F_{H,0}^S}$$

Tube side:

Using similar manner, the following equations for the tube side can be obtained.

$$F_H^T \big|_z - F_H^T \big|_{z+\Delta z} = -\left(F_H^S \big|_z - F_H^S \big|_{z+\Delta z} \right)$$

(F-5)

$$\frac{dF_H^T}{dz} = -\frac{dF_H^S}{dz}$$

(F-6)

$$\frac{d\Phi_H^T}{dL} = -\frac{d\Phi_H^S}{dL}$$

(F-7)

The dimensionless molar flow rate of H_2 in tube side, Φ_H^T, can be derived in term of dimensionless molar flow rate of H_2 in tube side.

$$\int_0^{d\Phi_H^T} d\Phi_H^T = -\int^{d\Phi_H^S} d\Phi_H^S$$

$$\Phi_H^T = \left(1 - \Phi_H^S \right)$$

(F-8)

Eq.F-4 and F-8 were used to simulation compared with experimental data to determination of hydrogen permeability coefficient (α_H) of Eq.F-4
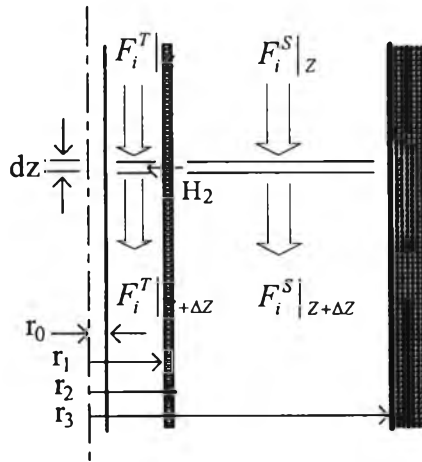
APPENDEX G

MEMBRANE REACTOR MATHEMATICAL MODEL

A schematic representation of the membrane reactor used in the development of the mathematical models is given in Figures G-1 and G-2. Two membrane reactor models were considered namely models with and without radial effect. Details are discussed as follows.

A. Plug flow model

Assumption:

- Steady state operation
- Isothermal operation
- Negligible thermal and concentration gradients in the catalyst pellets.
- Negligible radial diffusion effect.

Figure G-1 Schematic diagram of mass balance of plug flow model.

Shell side :

A steady state mole balance on product i in the reactor segment between z and z + Δz is:

$$F_i^S\big|_z - F_i^S\big|_{z+\Delta z} = J_H 2\pi r_2 \Delta Z - v_i \rho_{cat} r_A' A_C^S \Delta Z \qquad (G-1)$$

where $J_H = \alpha_H \left(\sqrt{p_H^S} - \sqrt{p_H^T}\right)$ $\qquad (G-2)$

then; $\dfrac{dF_H^S}{dz} = v_i \rho_{cat} A_C^S k_{app}\left(p_{C_3H_8} - \dfrac{p_{C_3H_6} p_{H_2}}{K_{eq}}\right) - 2\pi r_2 \alpha_H \left(\sqrt{p_H^S} - \sqrt{p_H^T}\right)$ $\quad (G-3)$

Dimensionless form:

Eq.G-3 can be converted to a dimensionless form by basing molar flow rate of species i and bed length with initial total molar on shell side and total bed lengh, respectively.

$$\frac{d\Phi_i^S}{dL} = c_{S,1} \frac{\upsilon_i}{F_T^S} \left[\Phi_{C_3H_8} - \frac{\Phi_{C_3H_8}\Phi_{H_2}}{\left(\overline{F_T^S} K_{eq}/P^S\right)} \right] - c_{S,2}\alpha_i \left(\sqrt{\frac{\Phi_H^S P^S}{\overline{F_T^S}}} - \sqrt{\frac{\Phi_H^T P^T}{\overline{F_T^T}}} \right) \quad (G\text{-}4)$$

The pressure gradient dP/dz along the catalyst bed is calculated according to the Ergun equation

$$\frac{dP_T^S}{dz} = -150\frac{\mu v_z}{d_p^2}\frac{(1-\varepsilon)^2}{\varepsilon^3} - 1.75\frac{\rho v_z^2}{d_p}\frac{(1-\varepsilon)}{\varepsilon^3}$$

Tube side :

Similarly, the following equation for the tube side could be obtained:

$$F_i^T\big|_Z - F_i^T\big|_{Z+\Delta Z} = -J_H 2\pi r_2 \Delta Z \quad (G\text{-}5)$$

$$\frac{dF_H^T}{dz} = 2\pi r_2 \alpha_H \left(\sqrt{p_H^S} - \sqrt{p_H^T} \right) \quad (G\text{-}6)$$

Dimensionless form:

$$\frac{d\Phi_i^T}{dL} = c_{S,2}\alpha_H \left(\sqrt{\frac{\Phi_H^S P^S}{\overline{F_T^S}}} - \sqrt{\frac{\Phi_H^T P^T}{\overline{F_T^T}}} \right) \quad (G\text{-}7)$$
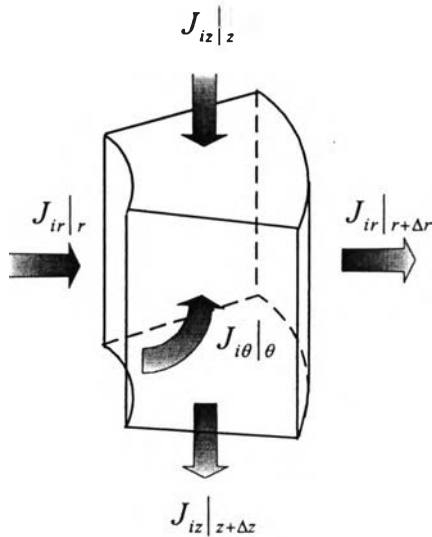
The dimensionless and constant terms are shown below.

$$\Phi_i^S = \frac{F_i^S}{F_{i,0}^S} \qquad\qquad c_{S,1} = l_0 A_c^S s\rho k P^S \ ,$$

$$\Phi_i^T = \frac{F_i^T}{F_{i,0}^S} \qquad\qquad c_{S,2} = \frac{2\pi r_2 l_0}{F_{T,0}^S} \ ,$$

$$\overline{F_T} = \frac{F_T}{F_{T,0}^S}$$

B. Radial flow model

Assumption:

- Steady state operation
- Isothermal operation
- Negligible pressure drop in catalyst bed
- Negligible thermal and concentration gradients in the catalyst pellets.

Figure G-2 Schematic diagram of mass balance of radial diffusion model.

Mole Balance

Mole balance on product i in the reactor segment between z and z + Δz, r and r + Δr, θ and $\theta + \Delta\theta$, is:

$$r\Delta r\Delta\theta\Delta z\frac{dC_i}{dt} = r\Delta r\Delta\theta\left(J_{iz}\big|_z - J_{iz}\big|_{z+\Delta z}\right) + \Delta r\Delta z\left(J_{i\theta}\big|_\theta - J_{i\theta}\big|_{\theta+\Delta\theta}\right) + \Delta\theta\Delta z\left(rJ_{ir}\big|_r - rJ_{ir}\big|_{r+\Delta r}\right) +$$

$$r\Delta r\Delta\theta\Delta z r_A \qquad\qquad\qquad\qquad (G-8)$$

then partial differential equation will be obtained:

$$-\frac{\partial C_i}{\partial t} = \frac{1}{r}\frac{\partial(rJ_{ir})}{\partial r} + \frac{1}{r}\frac{\partial J_{i\theta}}{\partial\theta} + \frac{\partial rJ_{iz}}{\partial z} - r_A \qquad\qquad (G-9)$$

In this case, the diffusion in z-component is ignored, then $J_{iz} = y_i \sum_{i=1}^{n} J_i = C_i u'$ (G-10)

and convection in r-component is ignored, then $\qquad J_{ir} = -\varepsilon D_{im}\frac{\partial C_i}{\partial r}$ (G-12)

Substitution Eq.10 and Eq.11 in Eq.9 a general partial differential equation at steady state condition is:

$$0 = \frac{\partial C_i u'}{\partial z} - \varepsilon D_{im}\left(\frac{1}{r}\frac{\partial C_i}{\partial r} + \frac{\partial^2 C_i}{\partial r^2}\right) - r_A \qquad\qquad (G-13)$$

A general partial different equation (Eq.G-13) is used to apply on membrane reactor system, PDE and its boundary condition are:

Shell side

$$\frac{\partial C_i u'}{\partial z} = \varepsilon D_{im}^S \left(\frac{1}{r} \frac{\partial C_i}{\partial r} + \frac{\partial^2 C_i}{\partial r^2} \right) + v_i \rho_{cat} k_{app} \left(p_{C_3H_8} - \frac{p_{C_3H_6} p_{H_2}}{K_{eq}} \right)$$

B.C. : $z = 0 ; C_i = C_{i,0}$

$$r = r_2 ; \frac{\partial C_i}{\partial r} = \frac{\alpha_i}{\varepsilon D_{im}^S} \left(\sqrt{p_H^S\big|_{r=r_2}} - \sqrt{p_H^T\big|_{r=r_1}} \right) \qquad \text{(G-14)}$$

$$r = r_2 ; \frac{\partial C_i}{\partial r} = 0$$

Tube side

$$\frac{\partial C_i u'}{\partial z} = D_{im}^T \left(\frac{1}{r} \frac{\partial C_i}{\partial r} + \frac{\partial^2 C_i}{\partial r^2} \right)$$

B.C. : $z = 0 ; C_i = C_{i,0}$

$$r = r_0 ; \frac{\partial C_i}{\partial r} = 0 \qquad \text{(G-15)}$$

$$r = r_1 ; \frac{\partial C_i}{\partial r} = \frac{\alpha_i}{\varepsilon D_{im}^T} \left(\sqrt{p_H^S\big|_{r=r_2}} - \sqrt{p_H^T\big|_{r=r_1}} \right)$$

Dimensionless form

The set of partial differential equations in Eq.G-3 was converted to dimensionless form by basing molar flow rate of species i and bed length with initial total molar on shell side and total bed lengh, respectively.

Shell side

$$\frac{\partial \Phi_i^S}{\partial Z} = b_{S,1} D_{im}^s P^S \left[\frac{1}{R^S - R_0^S} \frac{\partial}{\partial R} \left(\frac{\Phi_i^S}{F_T^S} \right) + \frac{\partial^2}{\partial R^2} \left(\frac{\Phi_i^S}{F_T^S} \right) \right] + \frac{b_{S,2} v_i P^S}{F_T^S} \left[\Phi_{C_3H_8}^S - \frac{\Phi_{C_3H_6}^S \Phi_{H_2}^S}{K_{eq} F_T^S / P^S} \right]$$

B.C. : $L = 0$; $\Phi_i^S = \Phi_{i,0}^S \quad (0 < R < 1)$

$$R^S = 0 ; \quad \frac{\partial}{\partial R} \left(\frac{\Phi_i^S}{F_T^S} \right) = \frac{a_{S,1} \alpha_i}{D_{im}^S P^s} \left(\sqrt{\frac{\Phi_i^S \overline{P}_T^S}{F_T^S}} - \sqrt{\frac{\Phi_i^T \overline{P}_T^T}{F_T^T}} \right) \qquad \text{(G-16)}$$

$$R^S = 1 ; \quad \frac{\partial}{\partial R} \left(\frac{\Phi_i^S}{F_T^S} \right) = 0$$

Tube side

$$\frac{\partial \Phi_i^T}{\partial Z} = b_{T,1} D_{im}^T P^S \left[\frac{1}{R^T - R_0^T} \frac{\partial}{\partial R}\left(\frac{\Phi_i^T}{\overline{F}_T^T}\right) + \frac{\partial^2}{\partial R^2}\left(\frac{\Phi_i^T}{\overline{F}_T^T}\right) \right]$$

B.C.: $L = 0$; $\qquad \Phi_i^T = \Phi_{i,0}^T \quad (0 < R < 1)$

$\qquad R^T = 0$; $\qquad \dfrac{\partial}{\partial R}\left(\dfrac{\Phi_i^T}{\overline{F}_T^T}\right) = 0$ $\hspace{5cm}$ (G-17)

$\qquad R^T = 1$; $\qquad \dfrac{\partial}{\partial R}\left(\dfrac{\Phi_i^T}{\overline{F}_T^T}\right) = \dfrac{a_{T,1}\alpha_i}{D_{im}^T P^T}\left(\sqrt{\dfrac{\Phi_i^S \overline{P}_T^S}{\overline{F}_T^S}} - \sqrt{\dfrac{\Phi_i^T \overline{P}_T^T}{\overline{F}_T^T}} \right)$

The dimensionless and constant term in Eq.G-16 and G-17 are:

$$\Phi_i^S = \frac{F_i^S}{F_{i,0}^S} \qquad\qquad \Phi_i^T = \frac{F_i^T}{F_{i,0}^S}$$

$$\overline{F}_T^S = \frac{F_T^S}{F_{T,0}^S} \qquad \overline{F}_T^T = \frac{F_T^T}{F_{T,0}^S} \qquad \overline{F}_{T,0}^S = \frac{F_{T,0}^S}{F_{T,0}^S} \qquad \overline{F}_{T,0}^T = \frac{F_{T,0}^T}{F_{T,0}^S}$$

$$\overline{P}_T^T = \frac{P^T}{P_0^S} \qquad \overline{P}_T^S = \frac{P^S}{P_0^S}$$

$$a_{s,1} = \frac{l_0 A_c^s \varepsilon}{(r_3 - r_2)^2}\left(\frac{\overline{F}_{T0}^S}{u_0^S P_0^S}\right) \qquad a_{s,2} = s\rho_{cat} k l_0 A_C^S\left(\frac{\overline{F}_{T0}^S}{u_0^S C_{T,0}^S}\right) \qquad a_{T,1} = \frac{l_0 A_c^T \varepsilon}{(r_1 - r_0)^2}\left(\frac{\overline{F}_{T0}^T}{u_0^T P_0^T}\right)$$

$$b_{s,1} = \frac{(r_3 - r_2)(P_0^S)^{3/2}}{\varepsilon C_{T,0}^S} \qquad b_{T,1} = \frac{(r_1 - r_0)P_0^T \sqrt{P_0^s}}{C_{T,0}^T}$$

APPENDIX H
PUBLISHED PAPER

These published paper emerged during this study were presented at Regional Symposium on Chemical Engineering, Songkla, November 22-24, 1999 and has been accepted on February 16, 2000 for publication in Journal of Chemical Engineering of Japan, Vol.33, No.3, 2000.

KINETICS FOR DEHYDROGENATION OF PROPANE

ON Pt-Sn-K/γ-Al$_2$O$_3$ CATALYST

SUTTICHAI ASSABUMRUNGRAT[1,3], WIROJ JHORALEECHARNCHAI[1],

PIYASAN PRASERTHDAM[1] AND SHIGEO GOTO[2]

[1] Petrochemical Engineering Laboratory, Department of Chemical Engineering, Chulalongkorn University, Bangkok 10330, Thailand

[2] Department of Chemical Engineering, Nagoya University, Chikusa, Nagoya, 464-8603, Japan

[3] To whom correspondence should be addressed.

Abstract

The performance of three catalysts, namely Pt/γ-Al$_2$O$_3$, Pt-Sn/γ-Al$_2$O$_3$ and Pt-Sn-K/γ-Al$_2$O$_3$ for dehydrogenation of propane is discussed. All catalysts are found to be highly selective towards propene. Pt-Sn-K/γ-Al$_2$O$_3$ appears to be the most stable and suitable catalyst for the dehydrogenation of propane. Pt-Sn/γ-Al$_2$O$_3$ is also found to be superior to Pt/γ-Al$_2$O$_3$. In the kinetic study, the reaction rate constants based on the number of active sites are calculated from the apparent reaction rate constants and the number of metal active sites. The reaction rate constants for Pt/γ-Al$_2$O$_3$, Pt-Sn/γ-Al$_2$O$_3$ and Pt-Sn-K/γ-Al$_2$O$_3$ catalysts at 773 K are 0.48×10^{-28}, 0.67×10^{-28} and 2.98×10^{-28} mol/(site.s.Pa), respectively. In addition, for Pt-Sn-K/γ-Al$_2$O$_3$, the frequency factor and the activation energy are 6.14×10^{-24} mol/(site.s.Pa) and 62.7 kJ/mol, respectively.

Introduction

The concept of membrane reactor has shown high potential for applications in the fields of biological and chemical reaction engineering during the past several decades. One of the major applications of membrane reactors is overcoming an equilibrium conversion by combining reaction and separation in a single unit operation. The dehydrogenation of propane to propene is one of the reactions of interest in this type of application. A number of researchers have studied this reaction using various types of membrane materials and catalysts. Sheintuch and Dessau (1996) used a Pd/Ru (or Pd/Ag) membrane reactor packed with a supported Pt catalyst. They found that the yield was limited by deactivation of the catalyst due to the low partial pressure of hydrogen in the reaction side. Weyten *et al.* (1997)

investigated the system using H_2-selective silica membrane with a chromia/alumina catalyst, and found that the propene yield was at least twice as high as the value obtained at thermodynamic equilibrium in a conventional reactor. Yildirim *et al.* (1997) evaluated the relative performance of three composite membranes; namely Pd/Ag, silica, and Pd-dispersed porous membranes. They found that the dense Pd-Ag composite system possessed higher performance levels. However, metal-dispersed porous systems had advantages due to their significantly higher contact surface-to-volume ratio.

Although significant research has been carried out in this area, there is little effort to investigate the reaction rate constants of propane dehydrogenation. This study is focused on kinetic determination for the dehydrogenation of propane. Three catalysts, namely $Pt/\gamma-Al_2O_3$, $Pt-Sn/\gamma-Al_2O_3$, and $Pt-Sn-K/\gamma-Al_2O_3$ were tested to find out the catalytic performance and the reaction rate constants were determined. These data are useful in the modeling of the dehydrogenation of propane in the membrane reactor.

1. Experiment

1.1 Catalyst preparation

$0.3\%Pt/\gamma-Al_2O_3$ catalyst was prepared by impregnation of a γ-alumina support.

γ-Alumina (produced by Sumitomo Alumina Smelting Co., Ltd., Japan) was ground to the desired mesh size, and then impregnated in a solution of chloroplatinic acid

dissolved in de-ionized water. The catalyst was heated at the rate of 10 K per minute, and calcined at 773 K for 3 h. 0.3%Pt–0.3%Sn/γ-Al$_2$O$_3$ catalyst was prepared by using an impregnation solution with mixtures of chloroplatinic acid and SnCl$_2$ dissolved in de-ionized water. 0.3%Pt-0.3%Sn-0.6%K/γ-Al$_2$O$_3$ could be made by re-impregnation of the calcined 0.3%Pt–0.3%Sn/γ-Al$_2$O$_3$ catalyst with potassium nitrate solution.

1.2 Carbon monoxide chemisorption technique

The metal active sites of fresh and used catalyst were measured using a carbon monoxide chemisorption technique whose concept is based on the assumption that one molecule of carbon monoxide adsorbs onto one metal active site (Burch *et al.*, 1994). Measurements were made using a pulse method. This technique involved pulsing a known volume of carbon monoxide over a catalyst sample at room temperature. The carbon monoxide that was not adsorbed was measured using a gas chromatography with a thermal conductivity detector. Pulses were continued until no further carbon monoxide adsorption was observed. The quantity of carbon monoxide adsorbed by the catalyst sample could then be calculated and hence the amount of metal active sites obtained.

1.3 Experiment

Dehydrogenation of propane was carried out in a micro reactor installed in a furnace with a temperature controller. The reactor was a quartz tube reactor whose inner diameter was 6.35 mm. The catalyst was packed in the middle of the quartz tube. Hydrogen gas was used to reduce the catalyst for 1 h, and then argon was used for purging hydrogen. The feed gas supplied by Thai Industrial Gases Limited was mainly a mixture of 3% propane in nitrogen. The experiment was performed at 773 K unless otherwise specified.

2. Kinetics

The rate equation for the dehydrogenation reaction can be expressed in the

following simple form

$$-r_A = k_{app}\left(p_A - \frac{p_B p_C}{K}\right)$$

$$= k_{app}\left(\frac{p_{Ao}(1-X_A)}{(1+y_{Ao}X_A)} - \frac{(p_{B0}+p_{Ao}X_A)(p_{C0}+p_{Ao}X_A)}{(1+y_{Ao}X_A)^2 K}\right) \tag{1}$$

By assuming a plug flow reactor, the apparent rate constant k_{app} can be determined as

$$k_{app} = \frac{F_{Ao}}{W}\int_0^{X_A}\frac{dX_A}{\left(\frac{p_{Ao}(1-X_A)}{(1+y_{Ao}X_A)} - \frac{(p_{B0}+p_{Ao}X_A)(p_{C0}+p_{Ao}X_A)}{(1+y_{Ao}X_A)^2 K}\right)} \tag{2}$$

The equilibrium constant, K can be calculated from Gibb's free energy data at different temperatures and correlated as the following expression.

$$K = 1.76 \times 10^{12} \exp(-15{,}521/T)$$
$$\tag{3}$$

3. Results and discussion

3.1 Comparison between catalysts

A set of experiment was carried out to compare the performance of Pt/γ-Al$_2$O$_3$, Pt-Sn/γ-Al$_2$O$_3$, and Pt-Sn-K/γ-Al$_2$O$_3$ catalysts. The conversion and selectivity to propene were measured as shown in **Fig. 1**. The propane molar flow rate was fixed at 6.24×10^{-7} mol/s, and the catalyst weight was 0.1 g.

All catalysts are highly selective towards propene, and the selectivities are higher than 95%. In addition, the conversions of all the catalysts decrease with time on stream, and reach the asymptotes after 120 min. Deactivation may be due to coke formation on the catalyst. The addition of Sn on Pt/γ-Al$_2$O$_3$ catalyst improves the

conversion of Pt/γ-Al₂O₃ catalyst. This can be explained by the ensemble effect in which the addition of Sn results in an increase in Pt dispersion and, hence, the stability of the catalytic activity is improved from the reduced amount of coke depositing on the metal active sites (Barias *et al.*, 1996; Krishnamurthy 1998). Moreover, the addition of Sn can improve the selectivity to propene due to blocking or poisoning of acid sites on the support (Barias *et al.*, 1995). Figure 1 also shows that Pt-Sn-K/γ-Al₂O₃ catalyst gives the highest conversion. This may be explained by three reasons, i.e.; (1) alkali metals such as potassium enhance hydrogen spillover on the catalyst surface; (2) alkali metals reduce the amount of coke depositing on the active sites (Praserthdam *et al.*, 1997); and (3) alkali metals neutralize the acid sites of the alumina support (Demiguel *et al.*, 1995).

3.2 Kinetic studies

As preliminary experiments, operating conditions where the resistances of external mass transfer and internal mass transfer are negligible were searched to obtain intrinsic kinetics. In this study, only Pt-Sn-K/γ-Al₂O₃ catalyst with the highest activity was tested. To investigate the effect of external mass transfer on the conversions, the experiment was carried out by using the same value of time factor, $W/F_{A,0} = 160$ s.kg /mol and the catalyst mesh size of 60–80 mesh. The feed flow rate was varied between 2.5-10.0 x 10^{-7} m³(STP)/s. The resistance of external mass transfer could be neglected when the feed flow rate was higher than 7.5x10^{-7} m³ (STP)/s. Another set of experiment was carried out to investigate the effect of internal mass transfer on conversion. Three ranges of catalyst sizes, 60-80, 200-250 and 250-

325 meshes, were tested under the same operating conditions such as the catalyst weight of 0.1 g, operating temperature of 773 K, and propane molar flow rate of 9.63×10^{-7} mol/s. The resistance of internal mass transfer was negligible for the catalyst size smaller than 60–80 mesh.

In order to determine the reaction rate constants, it was assumed that the decrease of catalyst activity was due to the formation of coke on metal active sites, and that the dehydrogenation of propane reached steady state within seconds (Larrson *et al.*, 1997, 1998). The experiment was carried out using 0.1 g of catalyst. The operating temperature was 773 K and the propane molar flow rate was 9.63×10^{-7} mol/s. **Table 1** summarizes the number of metal active sites of fresh catalysts and those of used catalysts after 3 and 120 min together with their corresponding conversions. The apparent reaction rate constants, k_{app} (calculated from Eq. (2)) at 3 and 120 min reaction times on stream are also presented in **Table 2**. It should be noted that the last column in Table 1 also provides some insight into the superior stability of the Pt-Sn-K/γ-Al$_2$O$_3$ catalyst by comparing the ratio of the metal active site of spent catalyst at 120 min (the values at the asymptotes) and of fresh catalysts, $N_{site,120\ min}/N_{site,fresh}$. It is clearly seen that the value of Pt-Sn-K/γ-Al$_2$O$_3$ catalyst is higher than the others. In other words, deactivation of the Pt-Sn-K/γ-Al$_2$O$_3$ catalyst is less than the other catalysts.

The reaction rate constants based on the number of active sites, k_{site}, is defined as follows.

$$k_{site} = k_{app}/N_{site} \qquad (4)$$

The values of the reaction rate constants, k_{site}, can be determined from the number of available active sites, N_{site} in Table 1 and are also presented in Table 2. The average reaction rate constant of Pt-Sn-K/γ-Al$_2$O$_3$ ($k_{site,aveage}$ = 2.98x10^{-28} mol/ (site.s.Pa)) is higher than those of Pt-Sn/γ-Al$_2$O$_3$ (0.67x10^{-28}mol/(site.s.Pa)) and Pt/γ-Al$_2$O$_3$ (0.43x10^{-28}mol/(site.s.Pa)). This implies that the presence of Sn does not significantly alter the strength of the metal active site while the presence of potassium increases the strength. This phenomena was also addressed previously by Demiguel (1995), where it was found that the addition of alkali metals produced a modification of the characteristics of the metallic phase which involved an electronic modification of the metallic phase.

To confirm the value of reaction rate constant of Pt-Sn-K/γ-Al$_2$O$_3$, one experiment was carried out using the same conditions except for a 20% mixture of propane in nitrogen. The obtained reaction rate constant of 3.08x10^{-28} mol/(site.s.Pa)) agrees well with that of 3% propane (2.98x10^{-28} mol/(site.s.Pa)).

To complete the kinetics for Pt-Sn-K/γ-Al$_2$O$_3$ the reaction rate constants were determined at different temperatures from 723 to 873 K. The obtained results fit very well with Arrhenius's equation as shown in **Fig. 2**. The following expression can be determined.

$$k_{site} = 6.14\text{x}10^{-24} \exp(-7,545/T) \tag{5}$$

The activation energy was 62.7 kJ/mol.

Conclusion

The performance of Pt/γ-Al$_2$O$_3$, Pt-Sn/γ-Al$_2$O$_3$ and Pt-Sn-K/γ-Al$_2$O$_3$ catalysts were investigated. All catalysts exhibit the selectivity towards propene higher than

95%. Pt-Sn-K/γ-Al$_2$O$_3$ appears to be the most suitable catalyst for dehydrogenation of propane. The reaction rate constant based on the number of metal active site for Pt/γ-Al$_2$O$_3$, Pt-Sn/γ-Al$_2$O$_3$ and Pt-Sn-K/γ-Al$_2$O$_3$ catalysts at 773 K are 0.43×10^{-28}, 0.67×10^{-28} and 2.98×10^{-28} mol/(site.s.Pa), respectively. Arrhenius's equation can be determined by changing temperatures.

Acknowledgement

Nomemclature

F_{Ao}	feed flow rate of propane	[(mol/s)]
k_{app}	apparent reaction rate constant	[mol/(kg.s.Pa)]
k_{site}	reaction rate constant based on active site	[mol/(site.s.Pa)]
K	equilibrium constant	[Pa]
N_{site}	number of active site	[site/kg]
p_i	partial pressure of component i	[Pa]
$-r_A$	rate of reaction	[mol.kg^{-1}.s^{-1}]
W	catalyst weight	[kg]
X_A	reaction conversion	[-]
y_{io}	initial mole fraction of component i in the feed inlet	[-]

Subscript

A	propane
B	propene
C	hydrogen
o	condition at feed inlet

References

Barias, O.A., A. Holmen and E.A. Blekkan; "Propane dehydrogenation over supported platinum catalysts - Effect of tin as a promoter," *Cat. Tod.,* **24,** 361-364 (1995)

Barias, O.A., A. Holmen and E.A. Blekkan; "Propane dehydrogenation over supported Pt and Pt-Sn catalysts: Catalyst preparation, characterization, and activity measurements," *J. Cat.,* **158,** 1-12 (1996)

Burch, R., P.J. Millington and A.P. Walker; "Mechanism of the selective reduction of nitrogen monoxide on platinum-based catalysts in the presence of excess oxygen," *App. Cat. B: Envi,* **4,** 65-94 (1994)

Demiguel, S.R., A.A. Castro, O.A. Scelza and J. Soria; "Effect of the addition of alkali-metals on the metallic phase of Pt/Al_2O_3 catalysts," *Cat. Letts.,* **32,** 281-291 (1995)

Krishnamurthy, K.R.; "Modifications in supported metal catalysts: Effect of promoters," *Recent Advances in Basic and Applied Aspects of Industrial Catalysis,* **113,** 139-150 (1998)

Larsson, M., N. Henriksson and B. Andersson; "Investigation of the kinetics of a deactivating system by transient experiments," *App. Cat. A,* **166,** 9-19 (1998)

Larsson, M., N. Henriksson and B. Andersson; "Estimation of reversible and irreversible coke by transient experiments," *Catalyst Deactivation,* **111,** 673-680 (1997)

Praserthdam, P., T. Mongkhonsi, S. Kunatippapong, B. Jaikaew and N. Lim; "Determination of coke deposition on metal active sites of propane dehydrogenation catalysts," *Catalyst Deactivation,* **111,** 153-158 (1997)

Sheintuch, M. and R.M. Dessau; "Observations, modeling and optimization of yield, selectivity and activity during dehydrogenation of isobutane and propane in a Pd membrane reactor," *Chem. Eng. Sci.,* **51**, 535-547 (1996)

Weyten, H., K. Keizer, A. Kinoo, J. Luyten and R. Leysen; "Dehydrogenation of propane using a packed-bed catalytic membrane reactor," *AIChE J.,* **43**, 1819-1827 (1997)

Yildirim, Y, E. Gobina and R. Hughes; "An experimental evaluation of high-temperature composite membrane systems for propane dehydrogenation," *J. Mem. Sci.,* **135**, 107-115 (1997)

Figure Captions

Figure 1 Conversion and selectivity with time on stream

$F_{A,0} = 6.24 \times 10^{-7}$ mol/s, $T = 773$ K, $W = 0.1$ g

$y_{A,0} = 0.03$, $p_{A,0} = 3039$ Pa, $p_{B,0} = p_{C,0} = 0$ Pa

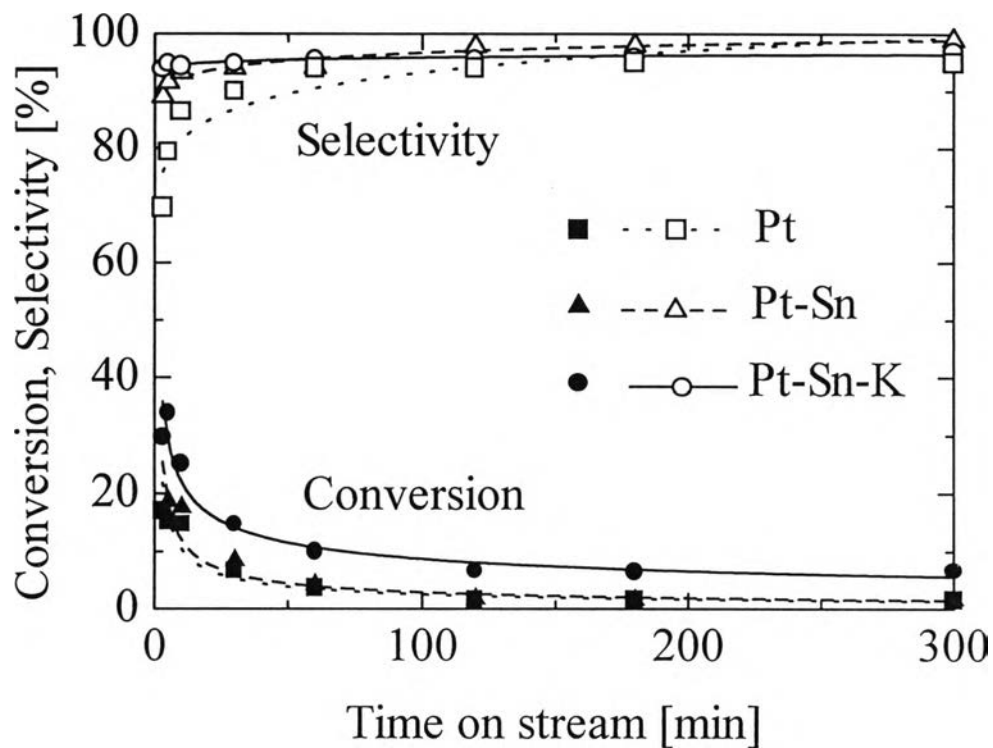**Figure 2** Arrhenius plot for Pt-Sn-K/ γ -Al$_2$O$_3$

Fig. 1   Conversion and seletivity with time on stream
$F_{A,0} = 6.24 \times 10^{-7}$ mol/s, $T = 773$ K, $W = 0.1$ g
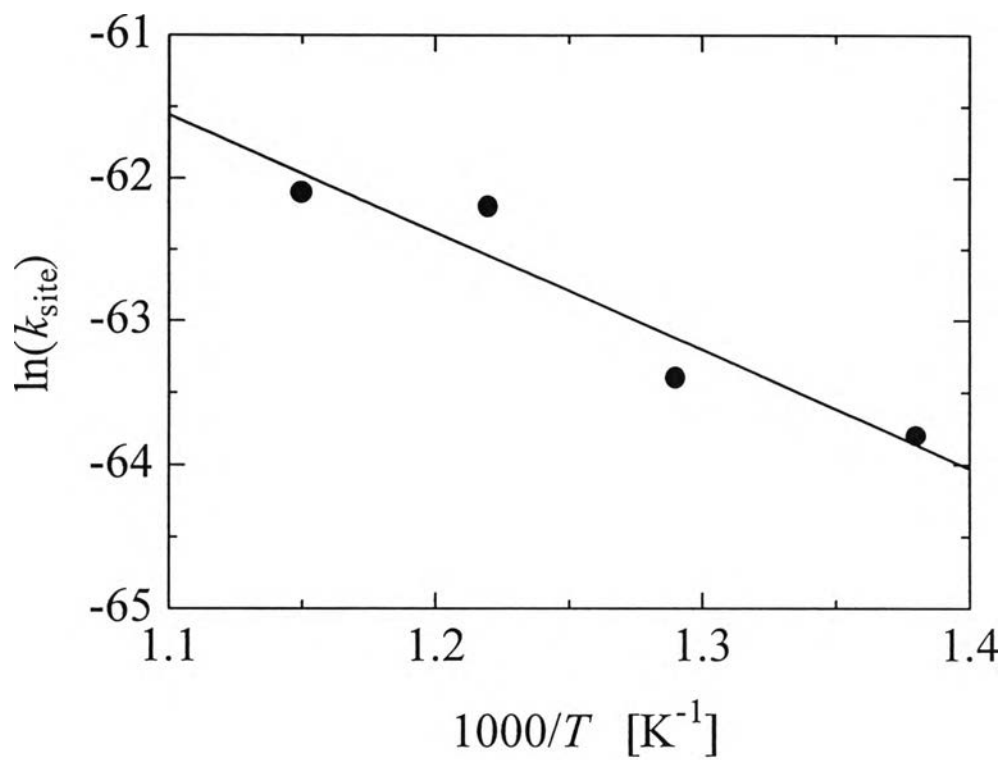$y_{A,0}$, $p_{A,0} = 3039$ Pa, $p_{B,0} = p_{C,0} = 0$ Pa

Fig. 2 Arrhenius plot for Pt-Sn-K/γ-Al$_2$O$_3$

Table 1 Values of $N_{site,fresh}$, $N_{site,3\ min}$, $N_{site,120\ min}$ and conversions at 3 and 120 min for three catalysts

Time	0 min	3 min		120 min		
Catalyst	$N_{site,fresh} \times 10^{-21}$ [site/kg]	Conversion [%]	$N_{site,3\ min} \times 10^{-21}$ [site/kg]	Conversion [%]	$N_{site,120\ min} \times 10^{-21}$ [site/kg]	$N_{site,120\ min}/ N_{site,fresh}$
Pt/γ-Al$_2$O$_3$	29.0	17.0	12.5	1.5	1.33	0.046
Pt-Sn/ γ-Al$_2$O$_3$	18.2	17.1	8.2	1.8	0.82	0.045
Pt-Sn-K/ γ-Al$_2$O$_3$	5.24	29.8	3.6	6.7	0.67	0.128

Table 2 Values of k_{app} and k_{site} for three catalysts

Time	3 min		120 min		
Catalyst	$k_{app,3\ min} \times 10^{7}$ [mol/(kg.s.Pa)]	$k_{site,3\ min} \times 10^{28}$ [mol/(site.s.Pa)]	$k_{app,120\ min} \times 10^{7}$ [mol/(kg.s.Pa)]	$k_{site,120\ min} \times 10^{28}$ [mol/(site.s.Pa)]	$k_{site,average} \times 10^{28}$ [mol/(site.s.Pa)]
Pt/γ-Al$_2$O$_3$	5.3	0.42	0.59	0.44	0.43
Pt-Sn/γ-Al$_2$O$_3$	5.7	0.70	0.54	0.64	0.67
Pt-Sn-K/γ-Al$_2$O$_3$	11.0	3.09	1.9	2.86	2.98

DEHYDROGENATON OF PROPANE IN A PALLADIUM MEMBRANE REACTOR

WIROJ JHORALEECHARNCHAI[1], SUTTICHAI ASSABUMRUNGRAT[1,3],
SHIGEO GOTO[2], PIYASAN PRASERTHDAM[1]

[1]Petrochemical Engineering Laboratory, Department of Chemical Engineering,
Chulalongkorn University, Bangkok 10330, Thailand
[2]Department of Chemical Engineering, Nagoya University,
Chikusa, Nagoya, 464-8603, Japan
[3]To whom correspondence should be addressed.

Abstract

The study consider the dehydrogenation of propane in a palladium membrane reactor. The study was divided into 3 main parts: the kinetics study of 0.3 wt%Pt- 0.3wt%Sn-0.6wt%K/γ-Al$_2$O$_3$ catalyst, the permeation study of hydrogen through a palladium membrane and the study on the membrane reactor. The Pt-Sn-K/γ-Al$_2$O$_3$ was selected because of its high resistance in catalyst deactivation. In the kinetic study, the effects of external and internal mass transfer were found to be negligible when the superficial velocity was higher than 1.6 m/s and the catalyst size was smaller than 60 – 80 mesh, respectively. The reaction rate constants for the Pt-Sn-K/γ-Al$_2$O$_3$ catalyst were determined by fitting the experimental results with a power-law kinetics at the reaction temperature ranging between 723-873 K. The reaction rate constant based on the active site at 773 K is 1.40×10^{-28} mol/(site s Pa). In addition, the frequency factor and the activation energy were 6.14×10^{-24} mol/(site s Pa) and 62.7 kJ/(mol K), respectively. The permeation study of pure hydrogen through a Pd-Ag membrane with 5 mm diameter and 0.1 mm thickness was carried at 573, 673 and 773 K. The permeation was assumed to follow Sievert's law. The obtained permeation coefficient at 773 K was 8.88×10^{-6} mol/(m^2 s Pa$^{0.5}$). The activation energy was and the frequency were 61.7 kJ/(mol K) and 0.11 mol/(m^2 s Pa$^{0.5}$), respectively. In the membrane reactor study, both mathematical modeling and experimental work were carried out. It was found that membrane reactor was superior to a conventional packed bed reactor and that the decrease of membrane thickness improves the performance of the membrane reactor.

Key Words: Dehydrogenation of propane, kinetics, hydrogen permeation, palladium membrane, membrane reactor

Introduction

The concept of membrane reactor has shown high potential for applications in the fields of biological and chemical reaction engineering during the past several decades. One of the major applications of membrane reactor is for overcoming an equilibrium conversion by combining reaction and separation in a single unit operation. The dehydrogenation of propane to propene is one of the reactions of interest in this type of applications. A number of researchers have studied this reaction using various types of membrane materials and catalysts. Weyten *et al.* (1997) investigated the system using H_2-selective silica membrane with a chromia/alumina catalyst. They found that the propene yield is at least twice as high as the value obtained at thermodynamic equilibrium in a conventional reactor. Yildirim *et al.* (1997) evaluated the relative performance of three composite membranes; namely Pd/Ag, silica and Pd-dispersed porous membranes. They found that the dense Pd-Ag composite system possessed higher performance levels in the temperature range studied. However, metal-dispersed porous systems have advantages due to their significantly higher contact surface-to-volume ratio.

The objective of this paper is to study the performance of membrane reactor. The kinetic of Pt-Sn-K/γ-Al$_2$O$_3$ catalyst which shows good resistance to deactivation by coking and high propane selectivity, and the permeation of H_2 were investigated to find reactor rate constants and permeation coefficients at different temperatures. In addition, a mathematical model was developed to simulate the performance of the membrane reactor.

Experiment

1. Catalyst preparation

0.3%Pt-0.3%Sn-0.6%K/γ-Al$_2$O$_3$ catalyst was prepared by dry-impregnation of 60 - 80 mesh γ-alumina support with an impregnation solution of chloroplatinic acid, stannous chloride and hydrochloric acid dissolved in de-ionized water. The catalyst was held at room temperature for 6 hours and dried overnight at 383 K. Next after calcining in air at 773 K for 3 hours at the heating rate of 10 K per minute. The catalyst was reimpregnated with potassium nitrate solution and recalcined to obtained the Pt-Sn-K/Al$_2$O$_3$ catalyst.

2. Kinetics study

The dehydrogenation of propane was carried out in a micro reactor installed in a electrical furnace with a temperature controller. The reactor is a quartz tube reactor whose inner diameter is 0.6 mm. 0.1 gram of catalyst with 60–80 mesh sizes was packed at the middle of the quartz tube. Hydrogen gas was used to reduce the catalyst for 1 hour and argon is for purging the system. The gas feed supplied by Thai Industrial Gases Limited was mixture of 3% propane in nitrogen. The propane molar flow rate was fixed at 2.37×10^{-7} mol/s. The experiment was performed at 773 K unless it will be specified in the text. Conversion and metal active sites at each time on stream were obtained using by gas chromatography and CO adsorption measurement.

3. Permeation and membrane reactor studies

Figure 1 shows the experimental setup for membrane reactor study. The membrane is made of Pd-Ag alloy with outer diameter 6 mm. The thickness of the separative palladium layer is 0.1 mm and the total length of the membrane 150 mm.

For the permeation studies, 16 grams of SiO_2 was packed inside the membrane tube. Pure H_2 was fed to the side while N_2 as a sweep gas was fed to tube side. Molar flow rate of H_2 was fixed at 2.46×10^{-5} mol/s that of N_2 was varied between 3.35×10^{-5} and 1.34×10^{-4} mol/s, respectively. Permeate and retentate flow rate was measured by bubble flow meters. For reaction studies, the experimental procedure was similar to the kinetic studies except it was carried out in membrane reactor and N_2 was used as sweep gas.
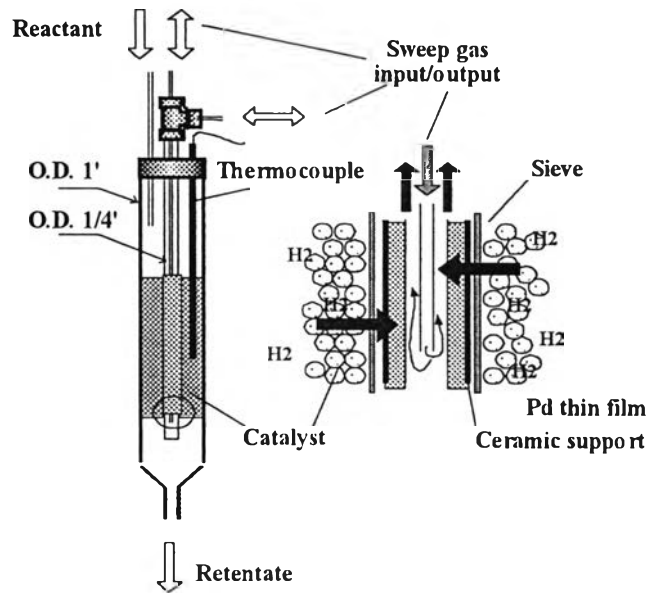

Figure 1. *Membrane module of Pd membrane reactor*

Results and discussion

1. Kinetics study

Rate expression

The rate equation for the dehydrogenation reaction is shown in Eq.1.

$$-r_A = k_{app} \left(p_A - \frac{p_B p_C}{K} \right) \tag{1}$$

$$= k_{app} \left(\frac{p_{Ao}(1 - X_A)}{(1 + y_{Ao} X_A)} - \frac{(p_{B0} + p_{Ao} X_A)(p_{C0} + p_{Ao} X_A)}{(1 + y_{Ao} X_A)^2 K} \right)$$

By assuming a plug flow reactor, the apparent rate constant k_{app} can be determined as

$$k_{app} = \frac{F_{Ao}}{W} \int_0^{X_A} \frac{dX_A}{\left(\dfrac{p_{Ao}(1 - X_A)}{(1 + y_{Ao} X_A)} - \dfrac{(p_{B0} + p_{Ao} X_A)(p_{C0} + p_{Ao} X_A)}{(1 + y_{Ao} X_A)^2 K} \right)} \tag{2}$$

Reaction rate constant

Before the determination of the reaction rate constants, the operating condition where the effect of external mass transfer and internal mass transfer are negligible must be investigated. It was found that the resistances of external and internal mass transfer could be neglected when the superficial velocity was higher than 1.6 m/s and the catalyst size was smaller than 60–80 mesh, respectively.

In order to determine the reaction rate constants, it was assumed that the decrease of catalyst activity was due to the formation of coke on metal active sites and that the dehydrogenation of propane reached steady state within seconds (Larrson *et al.*, 1997 and 1998). Conversion and selectivity of propylene shown in Fig.2 were used to calculate the apparent reaction rate constants, k_{app}, which reflect the rate constant at the corresponding number of available active sites, N_{site} as shown in Table1.

Taking into account only the available active sites, the reaction rate constants based of the number of active sites, k_{site}, is defined as follows.

$$k_{site} = k_{app} / N_{site} \qquad (3)$$

Table1. Available metal active sites and rate constants of Pt-Sn-K/γ-Al₂O₃ catalyst at 773K.

Time on stream (min.)	$N_{sit} \times 10^{-}$	$k_{ap} \times 10^{6}$ [mol/(kgcat*s*Pa)]	$k_{sit} \times 10^{28}$ [mol/(site*s*Pa)]
3	3.57	1.11	3.15
120	0.65	0.21	3.11
		Average	3.13

To complete the determination of the rate constant of the Pt-Sn-K/γ-Al₂O₃ the reaction rate constants were determined at different temperatures from 873 to 723 K. The Arrhenius's equation can be determined as follows.

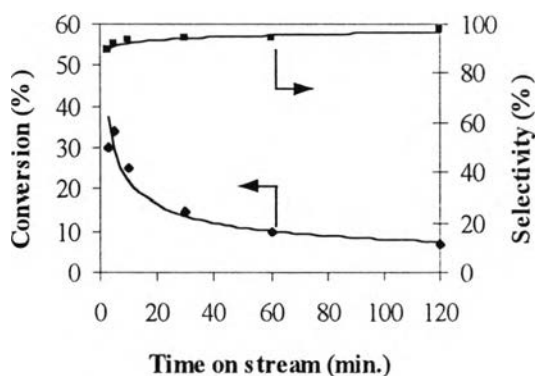$$k_{site} = 6.14 \times 10^{-24} \exp(-62,700/RT) \qquad (4)$$

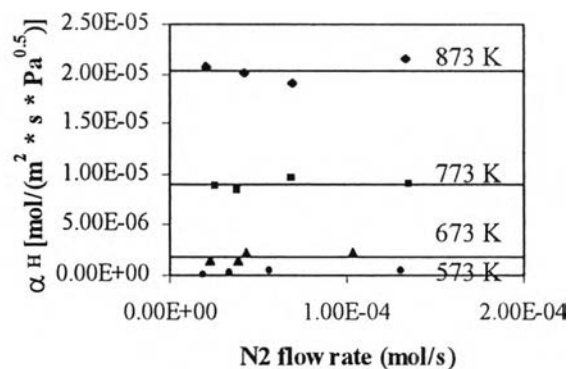Figure 2. Propane conversion and propylene selectivity at 773 K.

Figure 3. Permeation coefficient of H_2 (α_H) at 873,773,673 and 573 K.

2.Permeation study

Performing the material balance of hydrogen, a set of equations can be obtained :
For flow in the tube side

$$\frac{d\Phi_H^S}{dz} = -c\alpha_H \left(\sqrt{\beta^S} - \sqrt{\beta^T} \right)$$

(5)

For flow in the shell side

$$\frac{d\Phi_H^T}{dz} = -\frac{\Phi_H^S}{dz}$$

(6)

where

$$c = 2\pi r_2 Z_t \frac{\sqrt{P_0^S}}{F_{H,0}^S} \quad , \quad \beta^S = \frac{P^S}{P_0^S} \left[\frac{\Phi_H^S}{\Phi_H^S + \Phi_I^S} \right] \quad , \quad \beta^T = \frac{P^T}{P_0^T} \left[\frac{\Phi_H^T}{\Phi_H^T + \Phi_I^T} \right]$$

α_H is the permeability coefficient of hydrogen though the palladium membrane which was obtained by fitting the experimental results with the model. The amount of H_2 permeated through the Pd membrane was measured and used as one parameter in the permeation model. Fig. 3 show permeability coefficient with different N_2 sweep gas flow rate at 573,673,773 and 873 K. The continuous lines in the graph are the average value of α_H , it was found that the film resistance at the membrane interface at the N_2 side is not significant within the range of this study. The Arrhenius's equation can be determined as follow.

$$\alpha_H = 0.114\exp(-61,700/RT)$$

(7)

3. Membrane reactor

Mathematical model

To simplify the model for the membrane reactor, the following assumptions were made. The reactor is operated under plug flow regime and isothermal condition. In addition, the pressure drop in shell and tube side is negligible. Performing the material balance of catalyst bed, a set of equations can be obtained :
Shell side :

$$\frac{d\Phi_i^S}{dZ} = c_{S,1} \frac{\upsilon_i}{F_T^S} \left[\Phi_{C_3H_8} - \frac{\Phi_{C_3H_8}\Phi_{H_2}}{\left(\overline{F}_T^S/P^S\right)} \right] - c_{S,2}\alpha_i \left(\sqrt{\frac{\Phi_H^S P^S}{\overline{F}_T^S}} - \sqrt{\frac{\Phi_H^T P^T}{\overline{F}_T^T}} \right)$$

(8)

Tube side :

$$\frac{d\Phi_i^T}{dZ} = c_{S,2}\alpha_i \left(\sqrt{\frac{\Phi_H^S P^S}{\overline{F}_T^S}} - \sqrt{\frac{\Phi_H^T P^T}{\overline{F}_T^T}} \right)$$

(9)

where

$$c_{S,1} = z_t A_S s\rho k P^S \quad , \quad c_{S,2} = \frac{2\pi r_2 z_t}{F_{T,0}^S} \quad , \quad \Phi_i^S = \frac{F_i^S}{F_{i,0}^S} \quad , \quad \Phi_i^T = \frac{F_i^T}{F_{i,0}^S} \quad , \quad \overline{F}_T = \frac{F_T}{F_{T,0}^S}$$

Fig.4 shows the conversion of the membrane reactor from the both experiment and the simulation at different sweep gas flow rate. From the result, both values are comparative with the performance of membrane reactor was slightly improved when N_2 sweep gas flow rate was increased, Fig. 5 shows the simulation results when different of Pd-Ag alloy selective layer thickness were used. The simulated results deviate from the experiment ones within 5-10 % error. It was found that membrane reactor gives conversions exceeding the

equilibrium conversion and they are much increased when the membrane thickness was lower. In addition, the effect of sweep gas flow rate was more pronounced with the decrease of membrane thickness. The improvement of the conversion can be explained by the improved hydrogen removed hydrogen removal from the reaction chamber due to the increase of hydrogen pressure gradient with high sweep flow rate and the decrease of the membrane resistance with the thinner membrane thickness.
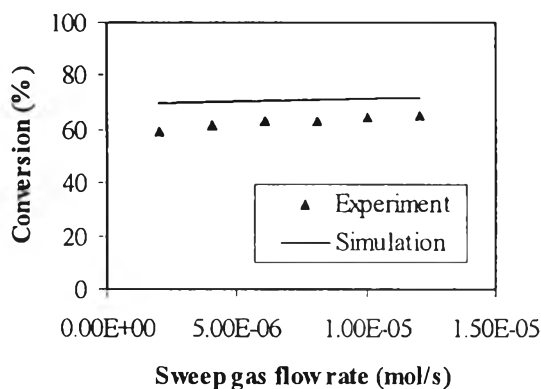

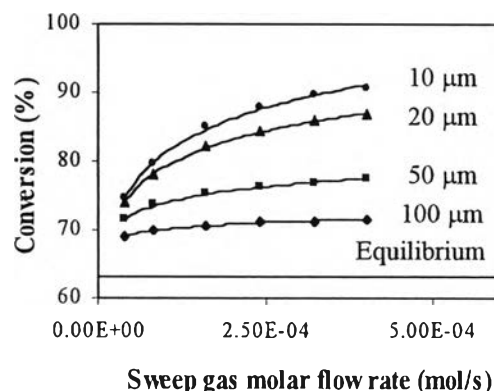Figure 4. Conversion of experiment and simulate study at 773 K.

Figure 5. Conversion of different Pd-Ag layer thickness at 773 K

Conclusion

The study of the gas phase dehydrogenation of propane in a membrane reactor has been carried out by simulating the mathematical model, whose parameters (rate constant and permeability coefficient) were obtained experimentally. Performance of membrane reactor could be approved over equilibrium conversion by using low Pd-Ag layer thickness and high sweep gas flow rate.

Acknowledgement

Nomenclature

A_s	=	Cross section area of bed [m^2]
F_I	=	Molar flow rate of species I [mol/s]
k_{app}	=	Rate constant (based on catalyst weight) [mol/(kg$_{cat}$*s*Pa)]
k_{site}	=	Rate constant (based on metal active site) [mol/(site*s*Pa)]
Keq	=	Equilibrium constant
N_{site}	=	Metal active site
P_i	=	Partial pressure [Pa]
P_T	=	Total pressure [Pa]
r	=	Membrane tube radius [m]
S	=	Metal active site per weight of catalyst [site/kg$_{cat}$]
X	=	Conversion

z_t	=	Membrane length [m]
α_H	=	Hydrogen permeability coefficient [mol/(m^2*s*Pa$^{0.5}$)]
ρ	=	Density of catalyst [kg$_{cat}$/m^3]
$\overline{F}_T$	=	Dimensionless total molar flow rate
Φ_i^S	=	Dimensionless molar flow rate of species I in shell side
Φ_i^T	=	Dimensionless molar flow rate of species I in shell side

Subscripts

A	=	Propane
B	=	Propene
C	=	Hydrogen
i	=	Component of mixture
0	=	Inlet value

Superscripts

S	=	Shell side
T	=	Tube side

References

Larsson M, N. Henriksson and B. Andersson. Investigation of the kinetics of a deactivating system by transient experiments. *App. Cat. A*, 166, 1998: 9-19.

Shu, J., Grandjean, B.P., Van Nestle, A. and Kaliaguine, S., Catalytic palladium-based membrane reactors: A review *Can. J. Chem. Engng* .vol. 69 ,1991:1036-1060.

Weyten, H., Keizer, K., Kinoo, A., Luyten., J. and Leysen, R. Dehydrogenation of propane using a packed-bed catalytic membrane reactor *AIChE J.* vol. 43, 1997 : 1819-1827.

Yildirim Y, E. Gobina and R. Hughes. An experimental evaluation of high-temperature composit membrane systems for propane dehydrogenation. *J. Mem. Sci.*,vol 135, 1997: 107-115.

VITA

Mr. Wiroj Jhonraleechanchai was born in Nakornrajchasrima on May 18, 1973. He received the Bachelor degree of science from the Department of Chemistry, Faculty of Science, King Mongkut's Institute of Technology Ladkrabang (KMITL) in 1997.